IDENTIFICATION OF ALKALI-SILICA REACTIVE FRAGMENTS IN SANDS AND GRAVELS, USING THE MORTAR BAR METHOD AND GEL PAT TEST, MODIFIED BY PETROGRAPHIC IMAGE ANALYSIS

Lukschová, Š*, Přikryl, R, and Pertold, Z

Institute of Geochemistry, Mineralogy and Mineral Resources, Faculty of Science,
Charles University in Prague, Albertov 6, 128 43 PRAGUE 2, Czech Republic

Abstract

The alkali-silica reactivity potential, of quartz sands and gravels, was determined using both the dilatational method (mortar bar test, according to ASTM C1260) and the modified gel pat test (higher concentration of alkaline solution, adjusted to less reactive particles, extended test period). Thin sections prepared from mortar bar and gel pat specimens were studied by optical microscopy, petrographic image analysis, and SEM/EDS analysis. In both types of test specimens, alkali-silica gels were observed in contact with quartzite fragments (quartz aggregates) and monomineral quartz fragments. In both types of specimens, the total volume of alkali-silica gel was positively correlated with the expansion measured by the mortar-bar method.

Keywords: alkali-silica reaction, aggregate, mortar bar method, gel-pat test, petrographic image analysis

1. INTRODUCTION

The alkali-silica reaction (ASR), first mentioned in the literature in 1940 by Stanton [1], is a solid-liquid heterogeneous chemical reaction of certain types of aggregates reacting in alkaline solution in concrete. The synergic effect of the following factors must occur: the presence of reactive forms of SiO_2, a sufficiently high enough concentration of alkaline ions, and the presence of moisture. The reaction product, alkali-silica gel, can absorb water molecules, which results in expansion. Consequently, this leads to mechanical failure in concrete [e.g. 2, 3].

The damage caused by ASR can be minimized by reducing the concentration of alkaline ions in cement, by preventing the input of water into the concrete, and by restricting the use of alkali-silica reactive aggregates in concrete. The first two approaches are hardly achievable for concrete exposed to atmospheric conditions, such as bridges or roads. Most of the test methods concerning ASR therefore focus on the determination of the aggregate reactivity. Tests can be divided into three groups: petrographic, chemical, and dilatometric [e.g. 4]. The petrographic method represents a less-frequently used method, although it has been adopted by several standards for the determination of the ASR potential of aggregates (e.g. TI-B52 [5], RILEM AAR-1 [6]). A simplified petrographic description classifies aggregates based upon the rock and/or mineral type, and according to generally accepted facts about their reactivity [e.g. 7, 8].

The alkali-silica reaction has become a widely discussed topic in the Czech Republic since the late 1990s, when the first damage to concrete was identified [9]. Over the past two decades, two major projects have been implemented to determine the alkali-silica reactivity potential of aggregates used in concrete [10, 11]. Additionally, new standard methods are being tested, and their possible application to Czech aggregates is being verified.

Gravel and sand are particulate detritus from weathering and erosion of igneous, metamorphic and/or sedimentary rock. The amount of quartz in the final detrital product increases with the number of (re-) iterations of erosion, transport and deposition, and can be significantly greater than in the original rock precursor. Gravel and sand are popular aggregate materials for concrete making [12]. The contribution of aggregates rich in crystalline quartz to the alkali-silica reaction has represented an unresolved research task for several decades [e.g. 13, 14].

1.1 Purpose of this study

This study focuses on the aspect of the alkali-silica reactivity of quartz sands and gravels, with the objective to verify the applicability of the gel pat test (Interpretation of petrographic analysis of aggregates in ASR, [15]), and the mortar bar method (ASTM C 1260 Accelerated

* Correspondence to: lukschova@seznam.cz, or: prikryl@natur.cuni.cz

mortar bar method [16]). The interpretation of the results of both tests has been improved by employing optical microscopy and petrographic image analysis.

The gel pat test was originally designed for the quick identification of opaline-rich aggregates [17]. Although it represents a feasible method, requiring a minimum of laboratory equipment and sample preparation, it is rarely used [e.g. 18, 19]. The greatest drawback of the entire method was pointed-out by Fournier and Berubé [19], who drew attention to the absence of quantification of the alkali-silica reactivity potential of aggregates in the gel pat method. The experimental conditions of this method are also unsatisfactory for most types of aggregates.

Accelerated mortar bar methods are frequently used to determine the alkali-silica reactivity of various types of aggregates. Their main advantages are: the short time period of the test, simple interpretation of the results, and possible comparison with other mortar bar tests. The impossibility of directly identifying the reactive particles is considered to be the major drawback of the method.

In this study, the gel pat test procedure was modified, particularly in relation to its possible application to quartz-rich aggregates. Macroscopic identification of alkali-silica gels was used in the preliminary stage of our study. All the samples investigated using the gel pat test were also tested according to ASTM C 1260. The measured expansion values were compared with the results from the gel pat test. The largest improvement, both optical and electron microscopy, as well as petrographic image analysis, was employed for a more detailed identification of alkali-silica gels (and in the identification of alkali-silica reactive aggregates in thin sections, prepared from mortar bar and gel pat specimens). Petrographic image analysis enabled quantification of the ASR potential of aggregates.

2 MATERIALS AND METHODS

2.1 Samples

The sands and gravels used in this study are petrographically classified as quartz sands and gravels. Their detailed petrographic characteristics are given elsewhere [20, 21]. Samples were taken from unconsolidated sedimentary deposits exploited within the Czech Republic (see Table 1), and used commercially as fine aggregates in concrete. Most of the deposits are connected to fluvial Quaternary sediments located around the Cidlina, Dyje, Labe, and Ploučnice rivers.

2.2 Modified gel pat test

The gel pat test [15] was originally designed to identify amorphous silica-rich aggregates, exhibiting rapid ASR in concrete and mortar. It enables detection of the ASR aggregates active in a special type of cement (CEM I 42.5). The gel pat test method consists of the following steps:

- *Sample preparation*. The bulk samples were separated by sieving into the following fractions: > 4 mm, 4/2 mm, and 2/0 mm. The 0.125/0 mm and > 4 mm fractions were not included. The gel pat specimens were prepared using the 4/0.125 mm fraction.
- *Gel pat specimen preparation.* A steel opening mould was used. The mould bottom was covered by aggregate fragments. The mortar was prepared using CEM I 42.5 Portland cement. The water/cement ratio equalled 0.40. The mortar was mixed and poured into the mould.
- *Gel pat specimen hardening.* After 24 hours of hardening, the gel pat surface containing aggregate particles was polished. The gel pat specimens were placed in plastic containers in alkaline solution. The containers were closed and maintained at room temperature.
- *Macroscopic examination.*

In this study, several parts of the gel pat test were modified:

- The originally designed size of the gel pat specimens (diameter 110 mm, height 25 mm) was reduced to a final size of 45 mm in diameter and 15-20 mm in height.
- The concentration of the alkaline solution was doubled, and calcium hydroxide was not added to the alkaline solution. The solution used in this study was 2 M (NaOH + KOH) solution.
- The accelerating period was prolonged, from 14 days to 20 days. Gel pat specimens were examined macroscopically.

2.3 Mortar-bar method

The ASTM C1260 accelerated mortar-bar method [16] is one of the most frequently used dilatometric methods employed in ASR classification of aggregates [13, 22, 23]. The preference for

this method is mainly as a result of the exact determination of the degree of ASR by dilatation values, its low cost, and its ease of use. ASTM C1260 classifies aggregates according to their dilatation value (Δ) into the following three following groups: I.) non reactive (Δ < 0.1%), II.) potentially reactive (Δ = 0.1 - 0.2%), III.) reactive (Δ > 0.2 %). The samples of sands and gravels were tested at ZKK s.r.o. Hořice, Czech Republic, using the ASTM C1260 accelerated mortar-bar method with the following steps:

- *Sample preparation.* The original samples were washed and dried at a temperature of 105 ± 5°C. The bulk samples were separated by sieving into the following fractions: > 4 mm, 4/2 mm, and 2/0 mm. The weight percentage of the individual fractions in each sample is shown in Table 1. The 0.125/0 mm fraction was excluded. The mortar-bar specimens were prepared using the 4/0.125 mm fraction.
- *Mortar-bar test specimen preparation.* The mortar-bar specimens were prepared using CEM I 42.5 Portland cement. After drying, the aggregate/cement ratio equalled 2.25. The water/cement ratio was 0.47. The mortar was mixed according to ČSN EN 196-1 and ČSN 72 2117. Two 25×25×285 mm test specimens were prepared from each sample.
- *Mortar-bar test specimen hardening.*
- *Dilatation value reading.* The lengths of the mortar bars were repeatedly measured every second day, and then the specimens were immediately moved back into storage containers filled with 1 N NaOH solutions maintained at 80°C. The containers were then placed in an oven heated to 80°C. The lengths of the mortar bars were repeatedly measured over a 14-day period.
- *Calculation of the total dilatation value.*

After the 14-day testing period, the mortar-bar test specimens were stored in air-proof plastic bags and were kept under wet conditions until the thin sections were prepared.

2.4 Optical microscopy and petrographic image analysis

Optical microscopy was performed using thin sections prepared (using a Struers Discoplan saw and Logitech WG2 polishing machine) from mortar bar specimens (3 sections for each specimen), and also from gel pat test specimens (2 sections per each specimen). The petrographic study of rocks and rock-like materials by optical microscopy and/or SEM/EDS constitutes an important part of aggregate ASR testing [e.g. 6], concrete damage mechanisms [3, 7, 24, 25]. Petrographic image analysis is a technique allowing quantification of ASR damage in concrete [26], the modal composition of rocks and/or the determination of their structural and textural characteristics [e.g. 27, 28].

Optical microscopy was employed for the basic description of the thin sections, including: the identification of the fragment type (petrography of coarse and fine aggregates), the relationship between aggregate and cement paste, and the type and location of voids and features related to the presence of alkali-silica gels. Moreover, a series of microphotographs were taken, and used later for the petrographic image analysis. A LEICA DMLP polarizing microscope (Optical Laboratory of the Institute of Geochemistry, Mineralogy and Mineral Resources, Charles University) was employed in this study. The microphotographs were taken on an Olympus Camedia C-2000Z camera, with 1600 × 1200 pixels.

The system of petrographic image analysis employed in this study consisted of manual image pre-processing, computer image analysis, and data evaluation. Image pre-processing involves: capturing of the image by means of conventional or digital photography in an optical microscope, identification of the measured objects (i.e. petrographic type of the fragments), and image modification using graphic software with a final image resolution of 300 dpi (Corel Draw v. 12.0).

The image modification is a crucial point in the image pre-processing, because the software used (SIGMASCAN Pro by Jandel Scientific) requires a binary image in which the object is differentiated from the background based upon the intensity along a grey scale. This means that the object must either be "lighter" or "darker" than the background. In the preparatory stage, it is also important to add an identifier to each object, indicating its petrographic nature. This identification is necessary for multiphase materials, such as the concrete samples studied. The analysis of multiphase materials requires measurement of an appropriate number of objects, which ranges from 200 to 300 per sample. Using SIGMASCAN Pro software, the image measurement is performed by a feature-specific approach (i.e. fill measurement). In practice, the objects are measured separately. After the measurement, each object is filled with a contrasting colour, in

order to avoid multiple analyses of an already-measured grain. Finally, the data obtained are analysed using any kind of statistical software. More details on the image preparation and image analysis can be found elsewhere [28].

2.5 SEM/EDS analysis on polished thin sections

The SEM/EDS analysis (a scanning electron microscope combined with an energy dispersive spectrometer) enables determination of the chemical composition of phases. During the past two decades, it has become the most useful technique used to investigate ASR products (white coatings covering the concrete surface, alkali-silica gels, e.g.) [7, 29]. During our study, the SEM/EDS method was used to verify the microscopic identification of selected phases, especially to identify alkali-silica gels. The uncovered polished thin sections were coated in a Carbon atmosphere. A Cambridge Cam Scan S4 electron microscope with an Oxford Instruments LINK ISIS 300 energy dispersive analytical system was used (Laboratory of Electron Microscopy and Microanalysis, Charles University, Prague). The measurement was carried-out under the following conditions: beam current 3nA, accelerating voltage 20kV, with 100nm resolution. A SPI Supplies 53 Minerals Standard set 02753-AB was used for routine quantitative calibration. The detection limit is 0.5 wt%.

3 RESULTS

3.1 Gel pat test

The number of reactive fragments was calculated during macroscopic observations of gel pat specimens. Every two days, the total number of reacting fragments was assessed and recalculated to a % (Table 2). During the first eight days, none of the samples studied exhibited signs of ASR. Alkali-silica reactive particles were observed in 4 out of 10 tested samples, after 14 days. The number of samples affected by ASR increased to 7 after 20 days of testing. In these 7 samples, the total number of alkali reactive particles varied between 5.0 and 18.2%.

3.2 Accelerated mortar bar test

The dilatation value (expansion) of the studied samples was measured using the ASTM C1260 (ASTM C 1260) mortar-bar method. The results for the studied samples are given in Table 3. The results of the mortar-bar test classify nine of the studied samples as non reactive (dilatation value < 0.100%). The same number of samples is classified as potentially reactive (dilatation value 0.100 – 0.200%), plus two samples are classified as reactive (dilatational value > 0.200%). Figure 1 shows the dilatation curves for all 10 samples studied with the limits for the reactive, potentially reactive, and non reactive classes.

3.3 Optical microscopy and petrographic image analysis of gel pat specimens

The more detailed modal composition of gel pat specimens was determined using conventional optical microscopy and image analysis (Table 4). Cement paste, monomineral, and rock fragments similar to those identified in a previous petrographic study represent major components of gel pat specimens. Alkali-silica gels and pores were observed in smaller amounts.

Alkali-silica gels were differentiated in the gel pat specimens into four different groups, according to their relationship to the surrounding phases:

I. Alkali-silica gel in contact with monocrystalline quartz fragments.
II. Alkali-silica gel in contact with polycrystalline quartz fragments.
III. Alkali-silica gel in contact with quartzite fragments.
IV. Alkali-silica gel in pores and cement paste (without any contact with sand fragments).

The presence of alkali-silica gels in contact with grains (monomineral or rock fragments) is considered to indicate the reactivity of the particular grains. In the case of alkali-silica gels of group IV, the alkali-silica gels are not connected with fragments. The amount of individual types of alkali-silica gels (Figure 2) was not calculated separately, due to its low volume. No alkali-silica gels were identified in contact with sedimentary, metasedimentary and granitoid rock fragments; or any in contact with monomineral feldspar grains.

3.4 Optical microscopy and image analysis of mortar bar specimens

The samples generally contain: monomineral clasts of quartz and feldspar; rock fragments of quartzite, sedimentary, and metasedimentary rocks (including phyllite, schist, and siltstone); granitoid rocks (including granite, quartz granite and granodiorite, volcanic fragments); pores and

cement paste. Various types of alkali-silica gels in various volumes were identified in 7 of 10 samples studied.

Alkali-silica gels (ASG) were differentiated according to their similar characteristics, as in gel pat specimens: ASG in contact with monocrystalline quartz fragments, ASG in contact with polycrystalline quartz fragments, ASG in contact with quartzite fragments, ASG in pores and cement paste (without any contact with sand fragments), and ASG in contact with more than one fragment ("spilt form"). No alkali-silica gels were identified in contact with sedimentary, metasedimentary, and granitoid rock fragments; nor in contact with monomineral feldspar grains.

4 DISCUSSION

4.1 Modification of the gel pat test method

The modified gel pat test represents a useful method in the determination of the alkali-silica reactivity potential of aggregates, and enabled a qualitative description of the samples studied, for the identification of individual minerals, as well as the quantification of the alkali-silica reactivity potential of aggregates.

The original version of the gel pat test method [15] requires only a 14-day test period, lower solution concentration, and macroscopic identification of alkali-silica reactive particles. All these aspects were modified in this study. The 14-day test period was found to be insufficient. The alkali-silica reaction was observed in contact with a small number of aggregates particles during this period. A higher number of aggregate particles reacted after this period (see Figure 3). The main cause of this problem could be seen in the material properties. The gel pat test was designed for opaline-rich samples, which react more rapidly and extensively than the sands and gravels used in this study (containing crystalline quartz particles).

4.2 Comparison of the results from the gel pat test with expansion values

The macroscopic identification of alkali-silica reactive particles and the modal composition of gel pat specimens were compared with the results of the mortar bar test (ASTM C1260, 21). This was done with the aim to quantify the alkali-silica reactivity potential of the tested aggregates.

Macroscopic identification of alkali-silica reactive particles correlates with the expansion value of the measured study samples, according to the ASTM C1260 mortar bar method (correlation factor R = 0.87, Figure 4, part a). A slightly higher correlation factor was obtained from the correlation of the expansion value with the precise quantification of the total volume of alkali-silica gels determined, using optical microscopy and image analysis (correlation factor R = 0.91, Figure 4, part b).

The alkali-silica reactive components of aggregates were identified according to their spatial connection with alkali-silica gels in gel pat specimens. On this basis, both quartzite and monomineral quartz fragments were considered to be reactive. The total volume of alkali-silica gel was correlated with the total volume of quartz and quartzite fragments; and no correlation was found (R = -0.02 in correlation with quartz, and R = 0.14 in correlation with quartzite fragments (Figure 5, part a, b)). A positive dependence of the total volume of alkali-silica gel on the volume of reactive quartz and quartzite particles (particles in contact with alkali-silica gel, denoted in Table 4 by A) was found; and higher correlation factors were calculated (R = 0.82 in correlation with quartz A, and R = 0.76 in correlation with quartzite A fragments (Figure 5, part (c, d)).

4.3 Optical microscopy of mortar bar specimens

Petrographic observations, similar to those performed on gel pat specimens, were employed for thin sections from mortar-bar specimens. The total volumes of the individual phases identified in the mortar-bar specimens were compared with the expansion (see Figure 6). All the calculated correlation factors (of linear or polynomial regression) are given in Table 6.

The highest correlation factor obtained (R = 0.96), in correlation of the expansion and total amounts of alkali-silica gels, confirms the fact that all the expansion behaviour of mortar-bar specimens is caused by ASR. Correlation factors calculated for other aggregates vary between 0.63 and 0.77. A more accurate correlation of polynomial regression and the regression curve, calculated for quartzite aggregates (Figure 6, part b), suggests the hypothesis about the pessimum effect of some types of aggregates, frequently discussed in the literature. The second possible explanation can be distinguished in the presence of different types of quartzite fragments, as was discussed in Lukschová et al. ([21], submitted).

A tighter correlation has been found for the expansion values plotted against the total sum of more than one phase identified in the mortar-bar specimens. All the phases contained in the

mortar bar specimens are accepted as possible factors affecting the expansion of the mortar bar specimens. In the first step, the influence of quartzite, sediment, and volcanic fragments is calculated (Figure 7, part a). In the second step, the influence of granitoids and feldspars was considered (Figure 7, part b). In the third step, quartz fragments were added (Figure 7, part c). In the last step, the influence of cement paste and pore voids is incorporated (Figure 7, part d). In conclusion, inclusion of more phases leads to a better correlation. The pessimum effect of aggregates can be seen when using polynomial regressions.

4.4 Questionable role of quartz aggregates in ASR

Commonly used petrographic standards (e.g. RILEM AAR-0) consider the angle of undulatory extinction of quartz grains to be the critical feature. All quartz grains with an angle of undulatory extinction higher than 15° are classified as reactive (or potentially reactive) in ASR. Numerous experimental studies were unable to confirm this hypothesis [13, 14, 22, 30, 31].

According to our previous results, the deformation and complete structural characteristics, grain size, and the presence and form (distribution) of minor minerals are considered to be the aggregate properties influencing ASR [21]. Both petrographic investigations carried out on gel pat and mortar bar specimens indicate large inaccuracies, when comparing the alkali-silica reactivity of aggregates (expansion or total volume of alkali-silica gels) with the total volumes of quartz and quartzite fragments. Quartz and quartzite alkali-silica reactivity could be variable; as was demonstrated in gel pat specimens, not all quartz and quartzite aggregates exhibit alkali-silica reaction.

5 CONCLUSIONS

The accelerated mortar bar method, modified by petrographic image analysis and optical microscopy, was successfully employed to determine the alkali/silica reactivity of low reactivity quartz sands and gravels. It combines four important aspects necessary for the assessment of reactive aggregates: I.) Aggregates are embedded in cement, II.) Their ASR potential is measured quantitatively using the expansion values and the total volumes of alkali-silica gels identified in mortar-bar specimens, III.) Alkali-reactive fragments are identified according to their spatial relationship with alkali-silica gel, IV.) The natural mineralogical and petrographic characteristics of aggregates can be described. Consequently, the modified mortar bar test minimizes potential observational errors.

The modified gel pat test method exhibits similar advantages (embedding of aggregates in cement, spatial relationship between reactive aggregates and ASR products). Modification of the solution concentration and the length of the testing period enabled application of the gel pat test to investigate sands and gravels containing crystalline quartz particles. Application of petrographic image analysis enabled semi-quantitative determination of the total amount of alkali-silica gels and alkali-reactive fragments. It is also possible to compare the results with the data for other types of aggregates.

6 ACKNOWLEDGEMENTS

This study was financially supported from the grant project of the Ministry of Transport of the Czech Republic (Project 1F45C/096/120), as well as project MSMT002160855 "Material Flow Mechanisms in the Upper Spheres of the Earth".

7 REFERENCES

[1] Stanton, TE (1940): Expansion of concrete through reaction between cement and aggregate. Proceedings of the American Society for Civil Engineering (66): 1781-1811.

[2] Powers, TC and Steinour, HH (1955): An interpretation of some published researches on the alkali-aggregate reaction. Part 1- The chemical reactions and mechanism of expansion. ACI Materials Journal (26/6): 497-516.

[3] St John, DA, Poole, AB and Sims, I (1998): Concrete petrography. A handbook of investigative techniques, Arnold Publishers, London: pp 474.

[4] Wang, H and Gillott, JE (1991): Mechanism of alkali-silica reaction and the significance of calcium hydroxide. Cement and Concrete Research (21): 647-654.

[5] ASTM C295-85 (1985): Standard practice for petrographic examination of aggregates for concrete. Annual Book of ASTM Standards. American Society for Testing & Materials. West Conshohocken.

[6] RILEM (2003): AAR-1 - Detection of potential alkali-reactivity of aggregates - petrographic method. Materials & Structures (36):480-496.
[7] Clark, BA, Swoeble, AJ, Lee, RJ and Skalny, J (1992): Detection of ASR in opened fractures of damaged concrete. Cement and Concrete Research (22): 1170-1178.
[8] Peterson, K, Gress, D, Van Dam, T and Sutter, L (2006): Crystallized alkali-silica gel in concrete from the late 1890s. Cement and Concrete Research (36/8): 1523-1532.
[9] Pertold, Z, Chvátal, M, Pertoldová, J, Zachariáš, J and Hromádko, J (2002): Damages in concrete pavement in highway D11 caused by alkali reactivity of aggregates. Beton (2): 21-24 (In Czech).
[10] Modrý, S, Dohnálek, J, Gemrich, J, Hörbe, M, Táborský, T and Dobiáš, D (2003): Elimination of alkali reactivity of aggregates in concrete in highway constructions. Unpublished technical report. Czech Technical University in Prague (In Czech).
[11] Pertold, Z, Lukschová, Š and Přikryl, R (2007): Identification of alkali-silica reactivity of aggregate in concrete and its causes. Unpublished technical report, Charles University, Prague. (In Czech).
[12] Prentice, JE (1990): Geology of construction materials. Chapman & Hall, London: pp216.
[13] Monteiro, PJM, Shomglin, K, Wenk, HR and Hasparyk, NP (2001): Effect of aggregate deformation on alkali-silica reaction. ACI Materials Journal (98/2): 179-183.
[14] Zhang, C, Wang, A, Tang, M, Wu, Z and Zhang, N (1999): Influence of aggregate size and aggregate size grading on ASR expansion. Cement and Concrete Research (29): 1393-1396.
[15] BS 7943 (1999): Interpretation of petrographic analysis of aggregates in ASR. British Standards Institution, London, UK.
[16] ASTM C1260 (1994): Potential alkali reactivity of aggregates (Mortar-bar method). Annual Book of ASTM Standards. American Society for Testing & Materials. West Conshohocken.
[17] Sims, I (1981): The Application and reliability of standard testing procedures for potential alkali-aggregate reactivity. In: Blight, GE (editor): Proceedings of the 5th International Conference on Alkali-Aggregate Reaction in Concrete, S252/13. Capetown. South Africa.
[18] French, WJ (1993): Independent geological assessment of Lamma Quarry as a source of concrete aggregate. Technical report. Taywood Maunsuell Ltd.
[19] Fournier, B and Bérubé, MA (1993): The use of the gel pat test to evaluate the potential alkali-reactivity of carbonate aggregates of the St. Lawrence Lowlands of Quebec. Cement and Concrete Composites (15): 49-73.
[20] Lukschová, Š and Přikryl, R (2006): Quantification of reactive components in sands and gravels by petrographic image analysis (modified RILEM method). In: Proceedings of the 2nd International Conference on Concrete Repair. St Malo, France.
[21] Lukschová, Š, Přikryl, R, Pertold, Z and Hörbe, M (submitted): Evaluation of the alkali-silica reactivity potential of sands: combination of dilatometric method and quantitative petrography of experimental specimens. Submitted to ACI Materials Journal.
[22] Grattan-Bellew, PE (1997): A critical review of ultra-accelerated tests for alkali-silica reactivity. Cement and Concrete Composites (19): 403-414.
[23] Kerrick, DM and Hooton, RD (1992): ASR of concrete aggregate quarried from a fault zone: Results and petrographic interpretation of accelerated mortar bar test. Cement and Concrete Research (22): 949-960.
[24] Lukschová, Š, Přikryl, R and Pertold, Z (2007): Petrographic examination of concrete from 20th century bridges and identification of reactive components. In: Proceedings of 5th International Conference on Arch Bridges. Funchal, Madeira, Portugal.
[25] Koskiahde, A (2004): An experimental petrographic classification scheme for the condition assessment of concrete in façade panels and balconies. Materials Characterization (53/2-4), Special Issue (29): 327-334.
[26] Rivard, P, Fournier, B and Ballivy, G (2000): Quantitative petrographic technique for concrete damage due to ASR: Experimental and application. Cement Concrete and Aggregates (22/1): 63-72.
[27] Siegesmund, S, Helming, K and Kruse, R (1994): Complete texture analysis of a deformed amphibole - comparison between neutron diffraction and U-stage data. Journal of Structural Geology (16/1): 131-142.
[28] Přikryl, R (2006): Assessment of rock geomechanical quality by quantitative rock fabric coefficients: Limitations and possible source of misinterpretations. Engineering Geology (87/3-4): 149-162.

[29] Fernandes, I, Noronha, F, and Teles, M (2007): Examination of the concrete from an old Portuguese dam: Texture and composition of alkali-silica gel. Materials Characterization (58/11-12), Special Issue (31): 1160-1170.
[30] Broekmans, MATM (2002): The alkali-silica reaction: mineralogical and geochemical aspects of some Dutch concretes and Norwegian mylonites. PhD-thesis Utrecht University, The Netherlands, pp 144.
[31] Hobbs, DW (1988): Alkali-silica reaction in concrete. Thomas Telford, London: pp183.

Table 1: Origin and cumulative grain size distribution of the studied materials.

S. no.	Deposit / Locality	Grain size distribution (mm)				
		>	4/2	2/0.1	<0.1	Total
179	Hradišťko I	3	4.0	57.8	0.9	100.0
181	Staré Ždánice	1	7.8	76.1	0.5	100.0
208	Roudnice - ACHP	4	9.2	48.4	2.0	100.0
279	Velký Luh	3	29.9	27.2	4.4	100.0
350	Pamětník	5	8.9	35.2	2.0	100.0
653	Roudnice - Sušice	2	13.5	61.3	0.8	100.0
668	Bratřice	2	13.1	82.4	1.9	100.0
676	Tasovice	7	12.5	75.4	4.8	100.0
1024	Provodín Jižní II	7	3.8	86.5	2.7	100.0
1027	Kaznějov	7	13.3	77.8	1.1	100.0

Table 2: Results from gel pat test.

Sample number	**179**	**181**	**208**	**279**	**350**	**653**	**668**	**676**	**1024**	**1027**
Total n. of fragments	**220**	**195**	**230**	**225**	**178**	**192**	**212**	**174**	**179**	**205**
Test duration in days	Number of reacting fragments in the testing period									
2	0	0	0	0	0	0	0	0	0	0
4	0	0	0	0	0	0	0	0	0	0
6	0	0	0	0	0	0	0	0	0	0
8	0	0	0	0	0	0	0	0	0	0
10	0	0	5	0	0	0	0	0	0	0
12	0	2	11	0	0	0	0	0	0	2
14	0	10	14	0	6	0	0	0	0	12
16	2	15	21	0	7	5	0	0	0	16
18	12	18	25	0	9	7	0	0	0	23
20	12	33	42	0	10	9	0	0	0	29
sample number	**179**	**181**	**208**	**279**	**350**	**653**	**668**	**676**	**1024**	**1027**
Test duration in days	Number of reacting fragments in % in the testing period									
2	0.0	0.0	0.0	0.0	0.0	0.0	0.0	0.0	0.0	0.0
4	0.0	0.0	0.0	0.0	0.0	0.0	0.0	0.0	0.0	0.0
6	0.0	0.0	0.0	0.0	0.0	0.0	0.0	0.0	0.0	0.0
8	0.0	0.0	0.0	0.0	0.0	0.0	0.0	0.0	0.0	0.0
10	0.0	0.0	2.2	0.0	0.0	0.0	0.0	0.0	0.0	0.0
12	0.0	1.0	4.8	0.0	0.0	0.0	0.0	0.0	0.0	1.0
14	0.0	5.1	6.1	0.0	3.4	0.0	0.0	0.0	0.0	5.9
16	0.9	7.7	9.1	0.0	3.9	2.6	0.0	0.0	0.0	7.8
18	5.5	9.2	10.9	0.0	5.1	3.6	0.0	0.0	0.0	11.2
20	5.5	16.9	18.3	0.0	5.6	4.7	0.0	0.0	0.0	14.1

Table 3. Dilatation values after a 14-day testing period.
TS1= test specimen 1, TS2 = test specimen 2. Expansion data in % ℓ/ℓ.

Sample no.		**179**	**181**	**208**	**279**	**350**	**653**	**668**	**676**	**1024**	**1027**
Exp. Δ (%)	TS1	0.132	0.210	0.192	0.042	0.136	0.186	0.024	0.028	0.044	0.220
	TS2	0.132	0.212	0.195	0.041	0.138	0.192	0.024	0.028	0.044	0.214
	Av.	0.132	0.211	0.194	0.041	0.137	0.189	0.024	0.028	0.044	0.217

Table 4. The modal composition of gel pat specimens determined by optical microscopy and image analysis. LLD - limits of detection; [1] - rocks with quartz amount higher than 95 wt. %; [2] - sedimentary and metasedimentary rocks including phyllite, schist, and siltstone; [3] - granite, quartz granite, and granodiorite; c.v.f. - crystalline volcanic fragments; g.v.f. - glassy volcanic fragments; A (resp. B) – fragments in (resp. without) contact with alkali-silica gel.

Sample no.	**179**	**181**	**208**	**279**	**350**	**653**	**668**	**676**	**1024**	**1027**
Quartz	10.00	21.80	21.60	28.60	17.80	13.50	23.00	4.36	32.28	20.98
Feldspars	-	-	-	-	0.73	-	1.20	6.34	-	-
Quartzite[1]	9.90	5.30	10.20	1.20	8.64	8.70	2.80	8.25	2.89	2.56
Sediment[2]	-	1.60		1.90	-	-	2.50	-	-	0.30
C.v.f. + G.v.f.	-	-	-	-	2.19	-	-	-	-	-
Granitoids[3]	1.43	4.10	3.87	-	4.90	4.60	3.50	22.16	-	-
Pores	LLD	0.30	0.60	0.20	LLD	0.20	LLD	LLD	0.40	0.20
Cement paste	78.19	65.80	62.00	68.10	65.22	72.30	66.90	58.80	64.40	73.70
Alkali-silica gel	0.50	1.20	2.10	LLD	0.80	1.00	LLD	LLD	LLD	1.90
Total	100	100	100	100	100	100	100	100	100	100
Quartz – A	6.50	8.70	12.60	7.60	10.10	13.50	5.80	4.20	5.40	14.90
Quartz – B	3.50	13.10	9.00	21.00	7.70	0.00	17.20	0.16	26.88	6.08
Quartzite1 – A	4.30	5.30	8.90	1.20	5.40	6.50	0.00	0.00	0.00	2.50
Quartzite1 – B	5.60	0.00	1.30	0.00	3.24	2.20	2.80	8.25	2.89	0.06

Table 5. The modal composition of mortar-bar specimens. LLD. = limits of detection;, P. – polycrystalline; M. – monocrystalline; fr. – fragment; [1] - rocks with quartz content higher than 95 wt. %; [2] - sedimentary and metasedimentary rocks including phyllite, schist and siltstone; [3] – granite, quartz granite, and granodiorite; [4] – alkali-silica gel in contact with polycrystalline quartz; [5] – alkali-silica gel in contact with monocrystalline quartz; [6] – alkali-silica gel in contact with quartzite; [7] – alkali-silica gel in cement paste and pores (without any contact with sand fragments); [8] – alkali-silica gel in spilt form, in contact with more than one fragment.

Sample no.	**179**	**181**	**208**	**279**	**350**	**653**	**668**	**676**	**1024**	**1027**
P. quartz	8.5	6.5	1.6	30.1	10.7	2.7	18.5	14.2	23.8	8.3
M. quartz	3.2	12.8	21.6	12.6	9.7	16.2	8.9	19.9	25.3	13.5
Feldspar	2.1	-	LLD	-	1.7	0.4	12.5	16.5	-	0.3
Quartzite[1]	15	12	12.9	16.5	19.3	18.2	LLD	0.6	3.4	15.7
Granitoid[2]	4	1.9	1.4	-	1.5	-	10.5	-	-	0.2
Sediment[3]	LLD	6.6	-	5.6	-	1.5	-	-	-	-
Volcanic fr.	2	-	-	-	0.5	-	-	-	-	-
Pores	9.9	3.9	1.5	1.2	2.1	8.2	3.2	6.8	3.9	7.1
Cement matrix	51.6	49.8	52.8	34	51	47.8	46.2	42	43.6	45.6
ASG[4]	0.4	0.3	-	-	0.3	LLD	-	-	-	0.6
ASG[5]	LLD	LLD	-	-	0.4	1	-	-	-	2.2
ASG[6]	0.5	5.4	-	-	2.5	3	-	-	-	4.3
ASG[7]	2.8	0.6	-	-	0.4	1.2	0.2	-	-	1.4
ASG[8]	-	0.1	8.1	-	-	-	-	-	-	1.0
Total	100	100	100	100	100	100	100	100	100	100
ASG - total	3.7	6.4	8.1	-	3.6	5.2	0.2	-	-	9.4
Quartz total	11.7	19.3	23.2	42.7	20.4	18.9	27.4	34.1	49.1	21.8

Table 6. Correlation factors R, calculated for correlation of the expansion values with the total volumes of the individual phases. ASG – alkali-silica gel; R_{lin} – correlation factor of linear regression; R_{pol} – correlation factor of polynomial regression; Quartz total – sum of monocrystalline and polycrystalline quartz; [1] – rocks with quartz content higher than 95 wt. %; [2] - granite, quartz granite, and granodiorite; r.f. – rock fragments.

Mineral / rock type	**Quartz**	**Feldspar**	**Quartzite[1]**	**Granitoid[2]**
Linear correlation R_{lin}	-0.70	-0.61	0.67	-0.28
Polynomial correlation R_{pol}	-0.70	-0.38	0.77	0.04
Phase	Volcanic r.f.	Pores	Cement paste	ASG
Linear correlation R_{lin}	0.06	0.22	0.63	0.96
Polynomial correlation R_{pol}	-	0.05	0.64	0.98

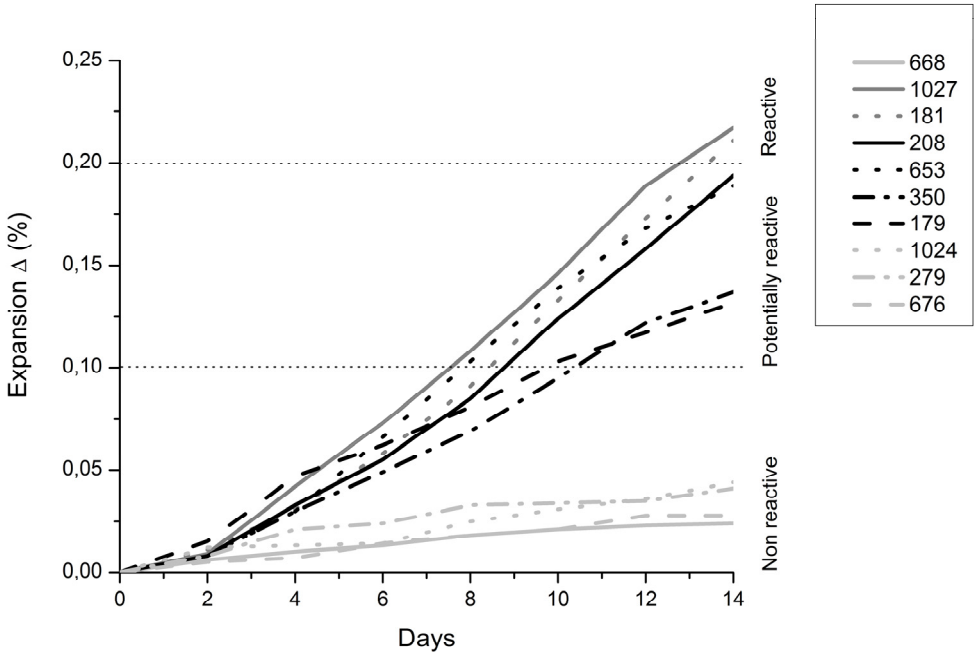

Figure 1: The dilatation curves of the studied samples (according to ASTM C1260).

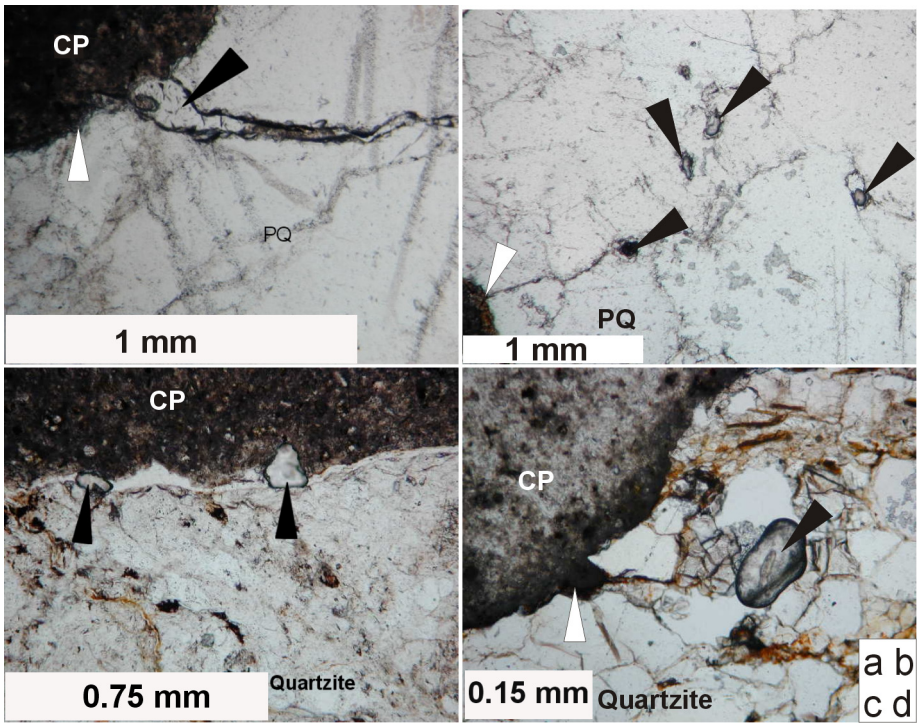

Figure 2: Micrographs of alkali-silica gels in gel pat specimens, in plane polarized light. Note different scale bars. Black arrows indicate alkali-silica gel; white arrows indicate aggregate boundary attacked by cement paste. CP – cement paste; PQ – polycrystalline quartz fragment.
(a) Crack filled by alkali-silica gel cutting through cement paste and quartz fragment.
(b) Polycrystalline quartz fragment damaged by cracks associated with alkali-silica gels.
(c) Crack along the cement-fragment boundary partially filled by alkali-silica gel.
(d) Quartzite fragment damaged by cracks associated with alkali-silica gel.

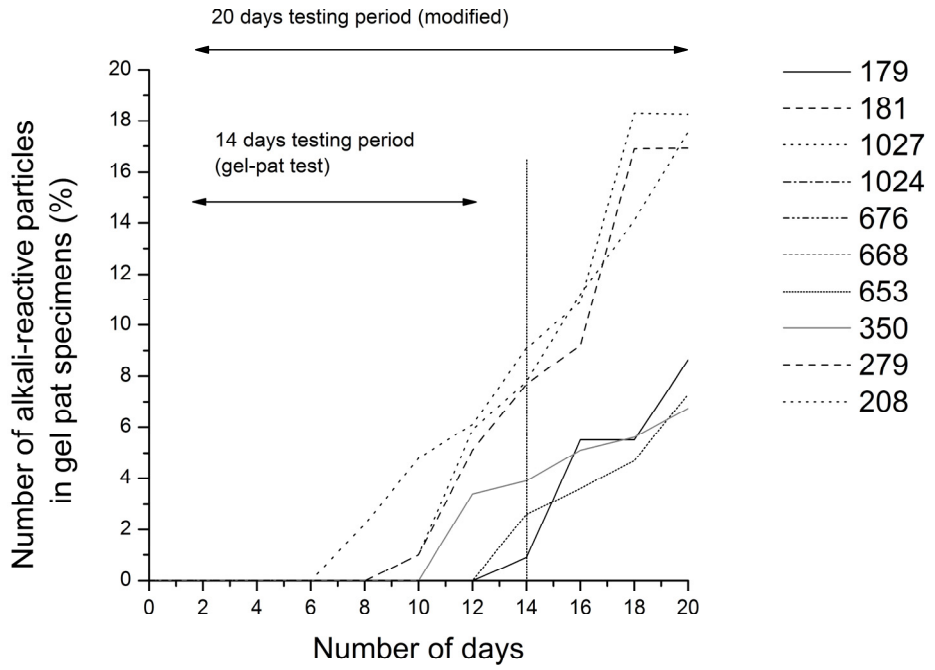

Figure 3: Number of alkali-silica reactive particles in gel pat specimens vs. exposure time in days.

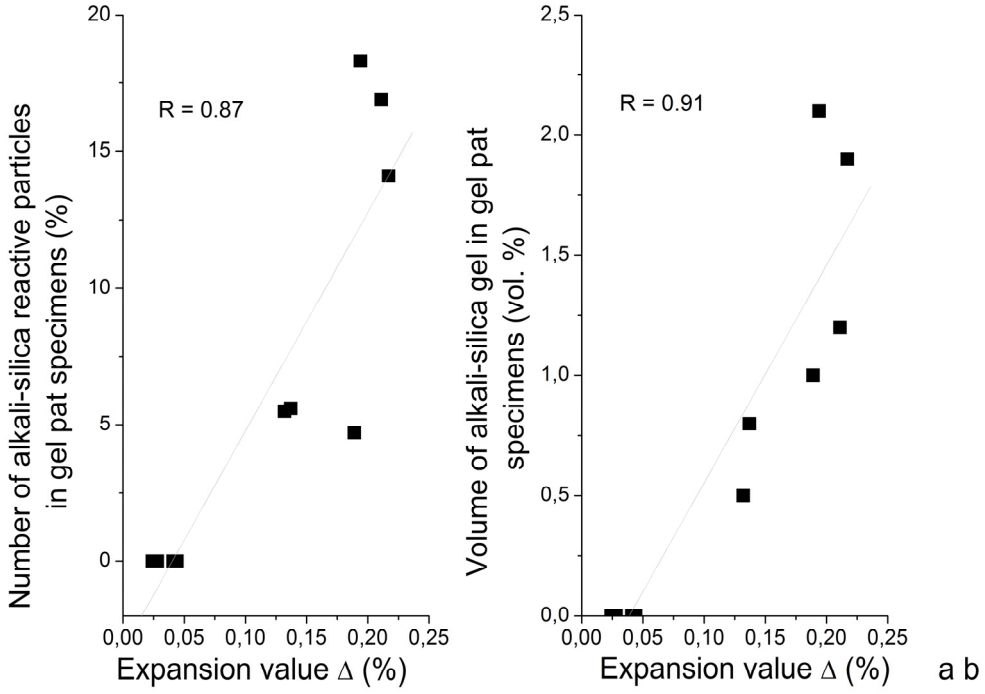

Figure 4: Comparison of expansion values (according to ASTM C1260), with the total number of alkali reactive particles in a gel pat specimen (part a, identified macroscopically); and total volumes of alkali-silica gels in a gel pat specimen (part b, by optical microscopy and image analysis).

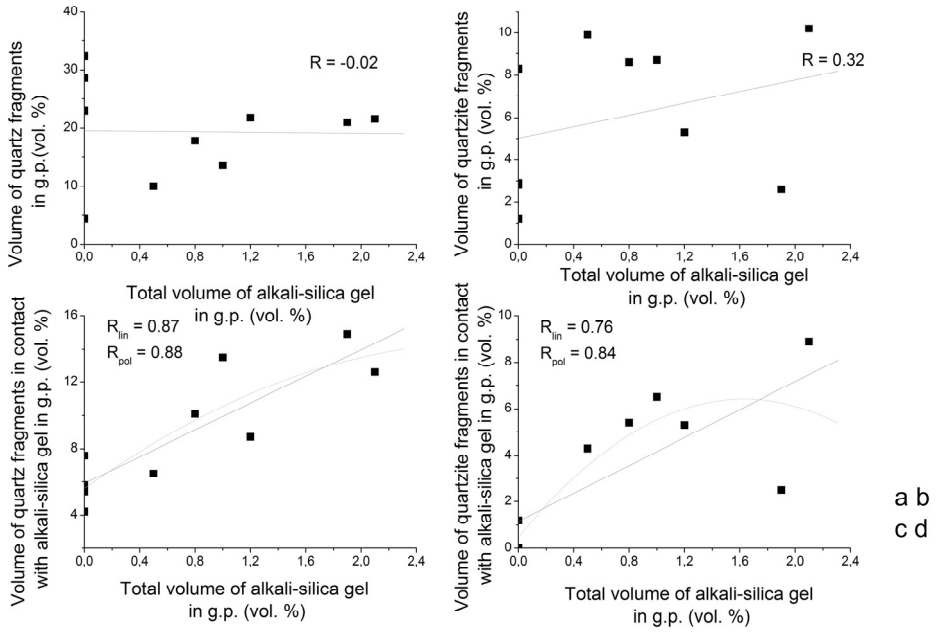

Figure 5: The gel pat test. Correlation of total volume of alkali-silica gel with the volume of quartz fragments (a); with quartzite fragments (b); with reactive quartz fragments (c); and with reactive quartzite fragments (d).

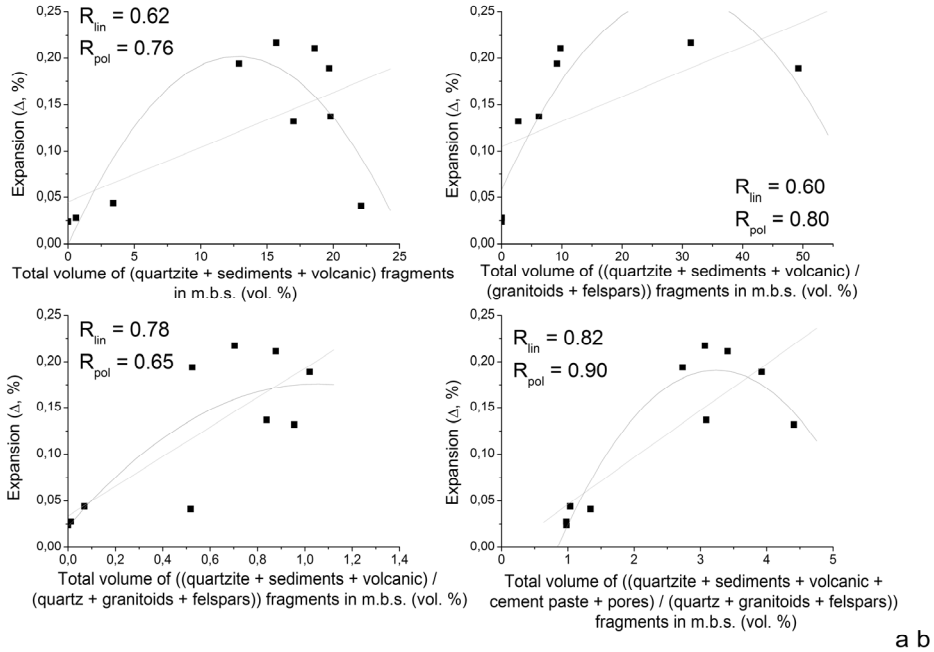

Figure 7: Correlation of the dilatation values (expansion) with the total volumes of (quartzite + sedimentary + volcanic) fragments (a); ((quartzite + sedimentary + volcanic) / (granitoid + feldspar)) fragments (b); ((quartzite + sedimentary + volcanic) / (quartz + granitoid + feldspar)) fragments (c); ((quartzite + sedimentary + volcanic + cement + pores) / (quartz + granitoid + feldspar)) fragments (d), in mortar-bar specimens (m.b.s.).

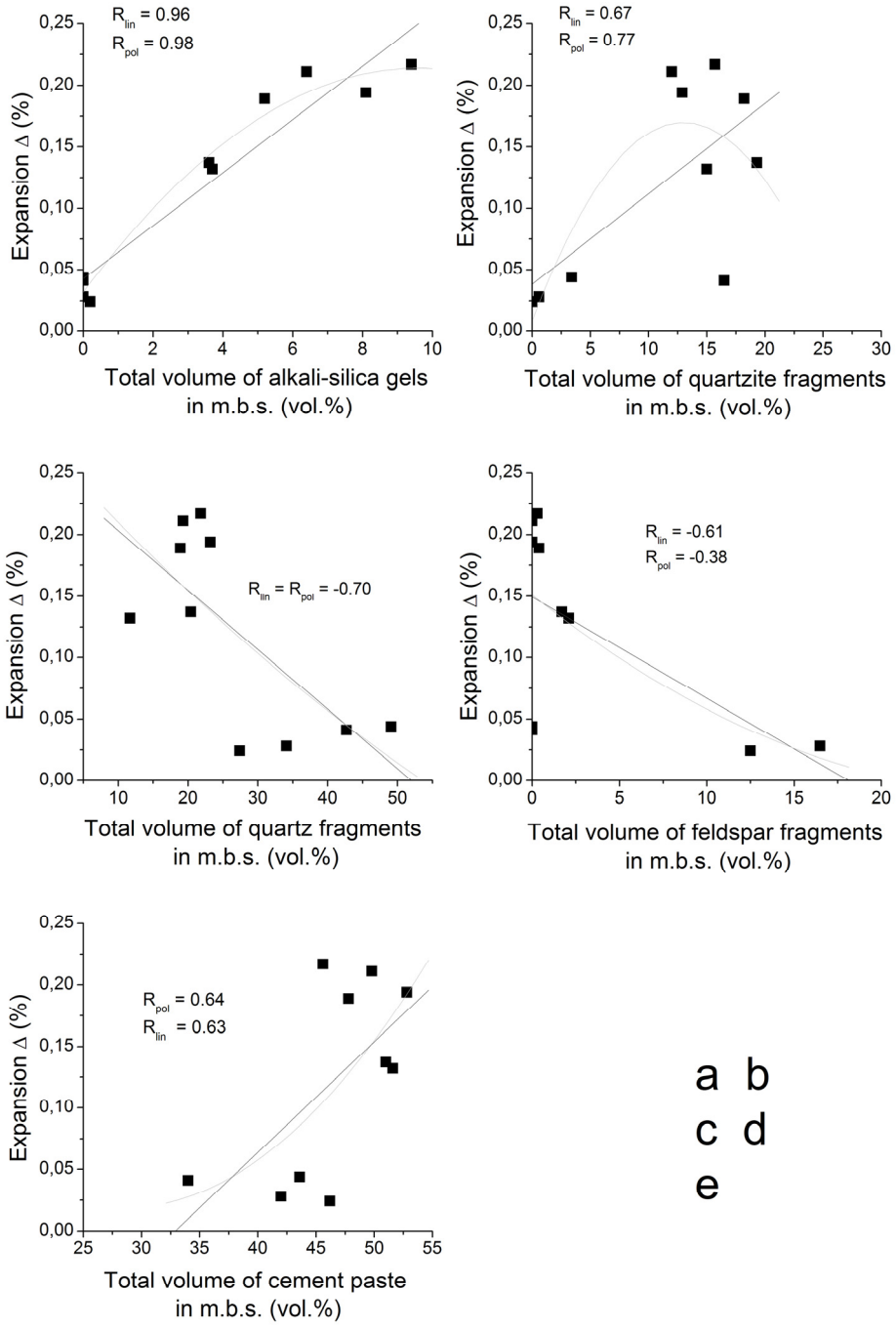

Figure 6: Correlation of expansion (Δ, % ℓ/ℓ) in mortar-bar specimens (m.b.s.) versus total volumes of: (a) alkali-silica gel, (b) quartzite fragments, (c) quartz fragments, (d) feldspar fragments, and (e) cement paste.